Journal Pre-proof

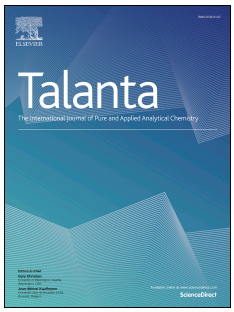

Sensing platform for pico-molar level detection of ethyl parathion using Au-Ag nanoclusters based enzymatic strategy

Deepika Sharma, Nishima Wangoo, Rohit K. Sharma

PII: S0039-9140(20)30558-0

DOI: https://doi.org/10.1016/j.talanta.2020.121267

Reference: TAL 121267

To appear in: *Talanta*

Received Date: 1 April 2020

Revised Date: 29 May 2020

Accepted Date: 31 May 2020

Please cite this article as: D. Sharma, N. Wangoo, R.K. Sharma, Sensing platform for pico-molar level detection of ethyl parathion using Au-Ag nanoclusters based enzymatic strategy, *Talanta*, https://doi.org/10.1016/j.talanta.2020.121267.

Credit Author Statement

Rohit K. Sharma : Corresponding author, Developed methodology, writing, editing and overall supervion of manuscript.

Deepika Sharma: Performed experiments and writing of manuscript.

Nishima Wangoo: Editing and supervision of manuscript development.

Graphical Abstract

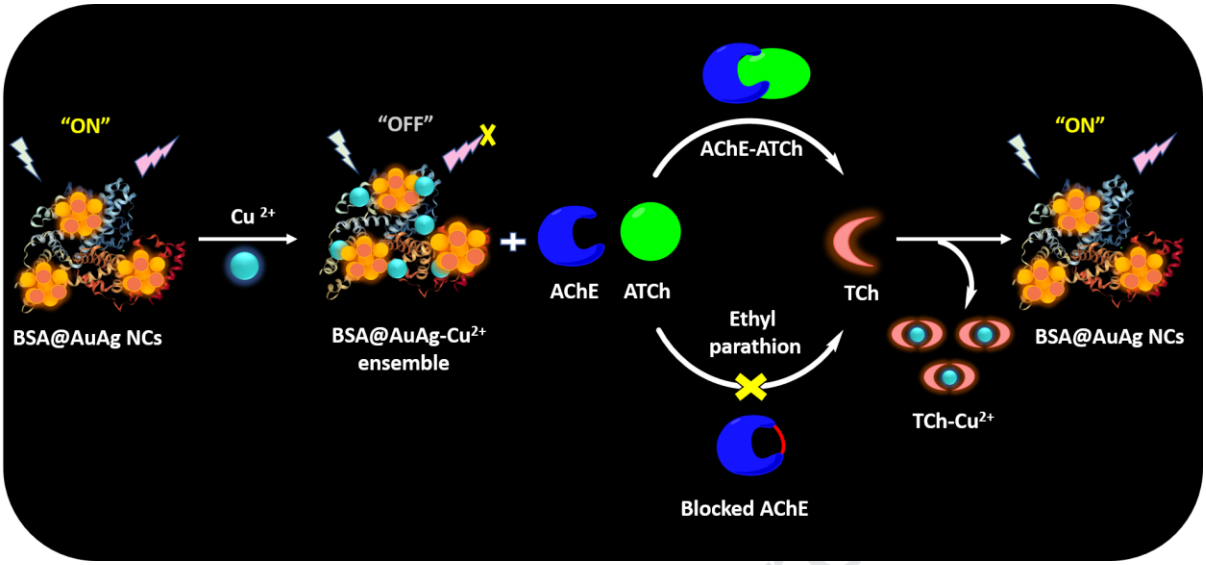

Sensing platform for pico-molar level detection of ethyl parathion using Au-Ag nanoclusters based enzymatic strategy

Deepika Sharma[a], Nishima Wangoo[b] and Rohit K. Sharma*[a]

[a]*Department of Chemistry & Centre for Advanced Studies in Chemistry, Panjab University, Sector-14, Chandigarh-160014, India*

[b]*Department of Applied Sciences, University Institute of Engineering & Technology (U.I.E.T.), Panjab University, Sector-25, Chandigarh-160014, India*

Graphical Abstract

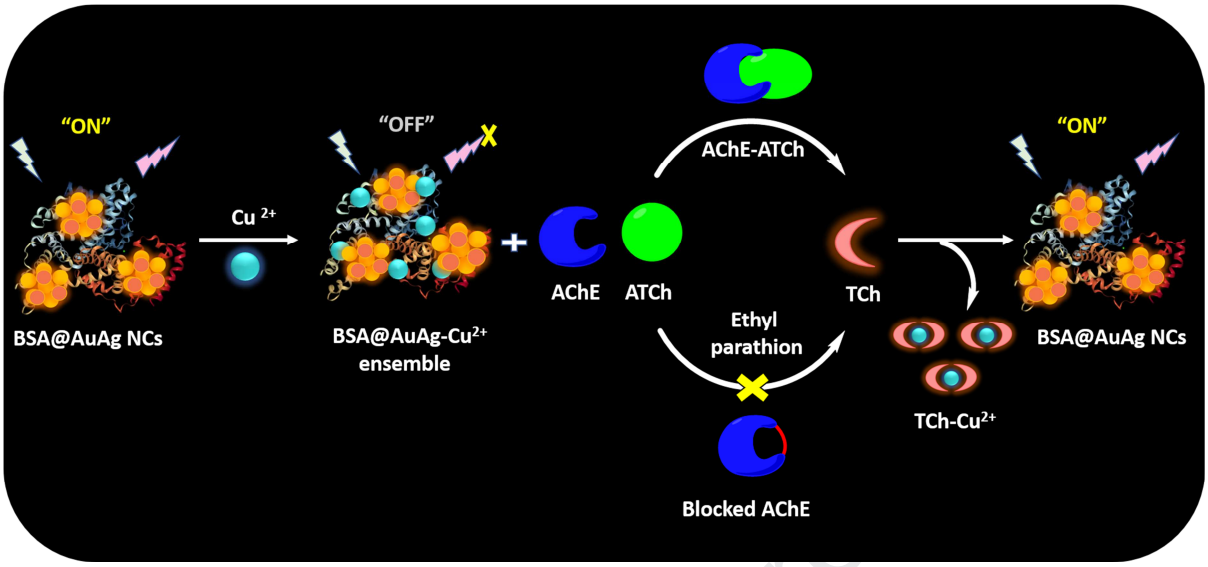

ABSTRACT

This work demonstrates a simple, cost effective and ultrasensitive detection of ethyl parathion, an organophosphorus (OPs) pesticide, using enzyme based fluorometric sensing strategy by employing bimetallic BSA@AuAg nanoclusters (NC). The sensing assay is based on the "quenched off" state of bimetallic NC with the addition of Cu^{2+} ions that can be "switched on" due to generation of thiocholine (TCh), a catalytic product of enzymatic reaction of acetylthiocholine (ATCh) using acetylcholinesterase (AChE) enzyme. The generated TCh preferably seize Cu^{2+} ions from BSA@AuAg NC-Cu^{2+} ensemble and recovered the fluorescence of BSA@AuAg NC. The presence of ethyl parathion can be monitored optically due to its inhibitory action towards AChE enzyme leading to suppression of thiocholine (TCh) formation and subsequently decreases TCh-Cu^{2+} interaction that ultimately retrieved quenched off state of bimetallic NC. The synthesized biosensor is appropriate for the ultrasensitive sensing of ethyl parathion in pM range, exhibiting 2.40 pM as lowest limit of detection (LOD) which is the least known so far. Further, the real sample analysis adds on for the appropriateness of the synthesized nanoprobe by depicting excellent reproducibility and robustness. The designed assay proved its specificity towards pesticides in general and ethyl parathion in particular when employed with other commonly used non-OPs pesticides.

KEYWORDS *BSA@AuAg NC; ethyl parathion; acetylcholinesterase; fluorescence; bimetallic nanoclusters; ultrasensitive detection.*

1. INTRODUCTION

The global usage of pesticides, in particular organophosphorus pesticides (OPs), has witnessed commercial benefits in terms of enhanced production of food and fibre over last few decades [1]. However, the prolonged usage of OPs has been associated with serious drawbacks of affecting the human health and also degrading the environment due to their long-term persistence in soil mainly owing to water solubility and easy absorptivity of these pesticides [2]. To make situation worse, it has been recently reported that the inevitable exposure to these pesticides has accounted for nearly 300,000 deaths annually [3]. Among different OPs, ethyl parathion (EP) which is commonly known as thiophos, is the one of the most widely used pesticides in agricultural as well as non-agricultural domains. Contrastingly, as per the environmental protection agency (EPA), ethyl parathion has been reported to be among the one of the most toxic chemicals registered in their directory [4]. The toxicity of ethyl parathion derives its origin from being an effective inhibitor to plasma, red blood cells and brain acetylcholinesterase (AChE) [5]. This inhibition leads to imbalance of acetylthiocholine (ATCh) amount, a neurotransmitter in central nervous system (CNS), giving rise to sensory and behavioral disturbances. Further, the ethyl parathion toxicity effects have been related to medical complications including Parkinson's disease, asthma, attention deficit and hyperactivity disorder (ADHD) as well as cancer when exposed for longer duration [6]. Considering these toxic effects, the maximum residue limit of ethyl parathion has been set at 0.01 ppm as per the European Union pesticides database [7]. Thus, the prevalent usage of ethyl parathion as a high-quality pesticide necessitates the consistent discovery and development of novel and more advanced detection strategies for its rapid, sensitive and effective quantification [8].

Among recent advancements in the area of OPs detection, the bio-substrate based sensors have been taking the forefront [9]. Especially, the sensing strategies based on utilizing the concept of AChE enzyme mechanism have demonstrated exceptional potential as a result of their ability to detect even a trace concentration of OPs when immobilized either electrochemically or optically [10-11]. In this context, approaches based on different traditional techniques such as gas chromatography-mass spectrometry (GC-MS), high performance liquid chromatography (HPLC), capillary electrophoresis etc. have been employed for pesticide detection, however, these have been reported to be associated with limitations that include requirement of high-cost instrumentation, long duration experimentation time and overall complex handling [12-14]. Approaches based on electrochemical techniques have also been employed for the selective detection of OPs in the past with ethyl parathion detection sensitivity as low as 40 nM [15-18]. However, such electro-analytical approaches have issues related to their stability, cleanliness, reusability and contamination of the electrode which are known to comprise their selectivity and sensitivity. Alternatively, $Ag@SiO_2$ nanospheres coupled with surface enhanced Raman scattering (SERS) has been utilized for ethyl parathion detection with relatively little success as the limit of detection (LOD) was observed in μM range [19]. Optical sensors fabricated by utilizing distinct surface plasmon resonance properties (SPR) of nanoparticles are found to be highly successful with ability of naked eyed visualization even for extremely low ethyl parathion concentration [20-23]. Specifically, ethyl parathion sensing assay using gold nanoparticles was reported by our group with detection sensitivity as low as 0.27 nM [24]. In search of more effective detection methods, newer techniques are being explored. One such recent report citing one-step direct competitive fluorescence enzyme (dc-FEIA) based method with LOD upto 0.68 nM for ethyl parathion [25]. However, this immunoassay required

relatively more cumbersome method for antibody generation and that too by trained personnel.

Fluorescence based optical signaling of OPs, in comparison to other techniques, has turned out to be more useful in terms of its relative simplicity, overall rapidness and ultra-sensitivity [26, 27]. Among various reports involving different fluorophores, enzymatic reaction modulated synthesis of CdTe quantum dots (QDs) have been recently utilized for detection of ethyl parathion as well as malathion with LOD of 1.3 nM and 4 pM, respectively [28-29]. Further, Forster resonance energy transfer (FRET) based sensors have been fabricated for ethyl parathion detection using carbon dots, though these require complex synthetic protocol, with high sensitivity of 585 nM [30]. Among fluorophores, metal nanoclusters (NC), having size less than 5 nm, have recently emerged as a viable alternative nanomaterial which can be employed in various application-based biosensors including usage as bio-labelling and bio-imaging probe [31]. Due to its ultrasmall size, metal NC exhibit distinct optoelectronics and chemical properties including strong photoluminescence, large stork shift and excellent photostability along with good biocompatibility [32]. Specifically, proteins/peptides-based approach for synthesis of metal NC is widely employed as their diverse functional groups offer a number of binding sites at ambient conditions and also eliminate the use of toxic reducing agent by acting as both reducing and capping agent [33]. The sensing applicability of NC has been already utilized for detection of different analytes such as Cr (VI) where microencapsulated photoluminescent metal NC were employed upto ppb level [34]. Similarly, bimetallic gold-silver (AuAg) NC confined in pomegranate silica type architecture were used for Cu^{2+} ion sensing through modulation of fluorescence intensity [35]. Thus, metal NC have been recently able to offer a highly sensitive alternative for the monitoring of analytes with different nature and properties [36]. Keeping this in mind, herein, bovine serum albumin (BSA) capped bimetallic gold silver nanoclusters (BSA@AuAgNC) were

synthesized and used for fluorometric detection of ethyl parathion owing to its strong luminescence. The detection assay involves interaction of Cu^{2+} ions with BSA@AuAgNC, leading to quenching of NC. The introduction of acetylcholinesterase enzyme (AChE), along with acetylthiocholine (ATCh) as a substrate, resulted in the generation of thiocholine (TCh) that preferably binds to NC bonded Cu^{2+} thereby re-enhancing the fluorescence intensity. The presence of ethyl parathion can be easily monitored using BSA@AuAgNC based proposed assay with calculated LOD in pico-molar range (2.40 pM). To the best of our knowledge, the present sensing strategy constitutes as the first report for the highly selective detection of ethyl parathion using bimetallic NC.

2. EXPERIMENTAL DETAILS

2.1. Chemicals and Reagents

Hydrogen tetrachloroaurate (III) trihydrate, silver nitrate, acetylcholinesterase, S-acetylthiocholine chloride and ethyl parathion were purchased from Sigma Aldrich India. Bovine serum albumin V (BSA), $CuCl_2.6H_20$ and sodium hydroxide were got from SRL India. For all the measurements and synthesis of BSA capped bimetallic Nanoclusters, ultrapure water having resistivity of 18.2 $M\Omega cm^{-1}$ was used taken from Direct Q3 system using Merck Millipore, India.

2.2. Synthesis of BSA capped bimetallic nanoclusters (BSA@AuAg NC)

The BSA@AuAgNCs were synthesized using a reported protocol with slight modification [37]. 10 ml of 0.3 mM of BSA was added into 10 ml of 4 mM $HAuCl_4.3H_2O$ solution followed by the addition of 4 mL of $AgNO_3$ (0.96 mM). After 10 min of stirring, 1 mL of 1 M NaOH solution was added dropwise and the reaction was allowed to continue for 16 h at 25 ^{0}C. The color of the solution changed to dark yellow indicating the formation of small

sized bimetallic NC (BSA@AuAg). The resulting clusters were purified using centrifugation at 7500 rpm to remove the unreacted BSA. The bimetallic NC were stored in dark at 4 ^{0}C.

2.3. Optimizations of proposed assay

2.3.1. Optimization for the determination of Cu^{2+} ions

The first step of the proposed scheme was the quenching of BSA@AuAg NC in the presence of Cu^{2+} ions. To carry out this step, 300 µL of stock solution of BSA@AuAg NC was added to different concentration of 40 µL of Cu^{2+} ions. The resulting mixture was incubated for 10 mins and subjected to fluorescence measurements.

2.3.2. Optimization for the ATCh substrate and AChE enzyme

The optimal concentration of ATCh was determined by observing its effect on the fluorescence intensity of BSA@AuAg NC. For this determination, different concentration of 100 µL of ATCh was added to 300 µL of BSA@AuAg NC followed by incubation and finally fluorescence intensity of BSA@AuAg NC was recorded. In the similar way, effect of AChE (10 µL) enzyme was also studied by recording the fluorescence intensity of BSA@AuAg NC (300 µL) in the presence of ATCh (15 µM, 100 µL).

2.3.3. Effect of pH on the proposed assay

pH played an important role in the enzymatic determination of ethyl parathion. In order to check the effect of pH for the detection of ethyl parathion, the enzymatic degradation of ATCh was observed in different pH conditions ranging from 4 to 11. The effect of pH was observed at the optimized parameters and conditions as stated above in section 2.3.1 and 2.3.2.

2.3.4. Optimization for the detection of ethyl parathion

Stock solution of ethyl parathion was prepared in methanol and stored at 4 ^{0}C. To validate the robustness of biosensor for the fluorometric determination of ethyl parathion, different concentration of ethyl parathion (100 µL) were added to AChE (10 µL, 300 mU mL^{-1}) in the presence of 50 µL of phosphate buffer solution (PBS) having pH =7.4. The resulting solution was incubated for 2.5 h at room temperature followed by the addition of ATCh (15 µM, 200 µL). Again, the mixture was incubated for 30 min at room temperature. Finally, the BSA@AuAgNC-Cu^{2+} solution was added and mixed for another 30 min. The fluorescence intensity was measured for BSA@AuAgNC at 650 nm.

2.4. Determination of ethyl parathion in spiked samples

The applicability of the proposed assay was determined by carrying out the analysis in real water and food samples. Tap water was used in its native form, whereas in case of soil water, it was filtered to remove suspended impurities and spiked with different concentration of ethyl parathion followed by its investigation using the above assay. Orange and apple juices were chosen to validate the practicability of biosensors in food samples. First of all, apple and oranges were cut and grinded to form homogenate solution followed by its filtration using 0.22-micron filter and finally diluted with water. Ethyl parathion was spiked in the food samples and determined using proposed assay.

3. RESULT AND DISCUSSION

3.1. Synthesis and characterization of BSA@AuAg NC

Fluorescent metallic NC have recently emerged as a new class of fluorophores that have attracted widespread attention owing to shrinkage of dimension comparable to Fermi wavelength of electrons [38]. The bimetallic NC have been extensively used over monoatomic clusters in order to utilize the synergic effect of both atoms for better optoelectronic performance [39-40]. The potential application of these NC in biomedical

applications can be achieved if they exhibit enhanced water solubility and biocompatibility along with high quantum yield. One of the ways to achieve this has been through usage of protein mediated synthetic approach for metal NC generation [41]. Among various proteins, BSA offers active site for the reduction and stabilization of the NC which helps to eliminate the use of toxic reducing agents [33]. In the present study, the bimetallic gold-silver (AuAg) NC were synthesized via one pot rapid biomineralization process using BSA which acted both as a scaffold and reducing agent. The synthetic protocol initially involved addition of gold (III) salt to the BSA solution resulting in the formation of BSA conjugated gold (BSA@Au) complex. This was followed by Ag (I) salt (in form of $AgNO_3$) addition to form BSA@AuAg complex at basic pH (12) (Figure 2) [37].

A broad peak of BSA@AuAg NC was obtained in the range of 300-350 nm in UV- Vis spectrum depicting a molecular type behavior which when measured along with $HAuCl_4$, $AgNO_3$, BSA and absence of any plasmonic peak eliminated the formation of large sized gold and silver nanoparticles [Figure S1 (A)]. The strong photoluminescence is the characteristic feature of these bimetallic NC due to quantum confinement effect. The fluorescence exhibited by the NC was mainly due to quantization of energy density state as a result of extremely small size of NC; thereby displaying emission at 650 nm wavelength upon excitation at 322 nm wavelength (Figure 2A). The synthesized BSA@AuAg NC were observed to be monodispersed in nature and exhibited spherical morphology as depicted in the HR-TEM image with the average size of about 5 nm (Figure 2B). Further, the hydrodynamic radius of the synthesized BSA@AuAg NC was about 8 nm [Figure S1(C)]. Also, the lattice plane revealed from X-Ray Diffraction (XRD) were (111) and (200) corresponding to sharp peak at 30.54^0 and 45.4^0 respectively [Figure S1 (B)] [42]. In addition to this, the nanocrystalline nature was also confirmed with well resolved lattice plane having spacing of 0.19 nm [Figure S2 (A, B)]. The presence of gold (Au), silver (Ag) and sulphur

(S) ion peaks in the EDX spectrum further confirmed the formation of BSA@AuAg NC [Figure S2 (C)]. The stability of NC can be attributed to the formation of Au-S bond (owing to presence of 35 cysteine residue in the BSA) along with the steric stabilization provided by bulkiness of protein. Also, it is quite well known that the tyrosine residues present in BSA gets deprotonated facilitating the reduction of Au salt to form small sized NC in highly alkaline medium.

3.2. BSA@AuAg NC based sensing statergy for the detection of ethyl parathion

The synthesized bimetallic BSA@AuAg NC were further employed as fluorescent nanoprobe for the detection of ethyl parathion, an organophosphorus pesticide (OP), using acetylcholinesterase enzyme (AChE) and acetylthiocholine (ATCh) as enzyme-substrate complex. Organophosphorus pesticides (OPs) are well known to inhibit the activity of AChE, a serine hydrolase enzyme which hydrolyzes the substrate ATCh to thiocholine (TCh) and acetate ion at a rate of 25,000 molecules of ATCh per second [5]. The toxicity of OPs in general and ethyl parathion in specific in is mainly due to their role in phosphorylation of AChE which leads to blockage of its catalytic site. Thus, this inhibitory action of ethyl parathion results in the accumulation of ATCh leading to initial sensory as well as behavioral disturbances with eventual fatal effect.

Keeping these toxic effects of ethyl parathion and its correlation with AChE-ATCh enzyme-substrate complex, we devised a fluorometry based novel strategy for ultra-sensitive detection of ethyl parathion. For this purpose, the synthesized BSA@AuAg NC exhibiting fluorescence at 650 nm [Figure 3A, 4A(i)] were quenched with the addition of Cu^{2+} ions (taken as $CuCl_2$) resulting in the formation of BSA@AuAg-Cu^{2+} ensemble, as a consequence, bimetallic NC showed complete quenching behavior [Figure 3A,4A(ii)]. The proposed ethyl parathion

detection assay was further devised into two pathways: one with absence of ethyl parathion (Path I) and other in the presence of ethyl parathion molecules (Path II). In the pathway I, AChE-ATCh complex was generated when AChE (300 mU/mL, 10 µL) interacted with ATCh (15 µM, 100 µL) which upon further hydrolysis led to the liberation of TCh. These TCh molecules were made to interact with previously generated BSA@AuAg-Cu^{2+} system through which it was observed that TCh preferably bound with Cu^{2+} ions (5 mM, 40 µL) from the system, due to strong binding affinity between thiol moiety of thiocholine and Cu^{2+} ions resulting into regainment of fluorescence intensity of BSA@AuAg NC [Figure 3B, 4A (iii)]. The TCh-Cu^{2+} complex formation can also be attributed on the basis of hard acid soft base (HSAB) principle [43]. On the contrary, the activity of AChE enzyme was blocked due to the introduction of even a trace level concentration of ethyl parathion (10 pM, 100 µL) that irreversibly bound with enzyme AChE, inhibiting its catalytic activity in pathway II rendering the ATCh molecules free. Due to non-presence of TCh or in other words due to absence of thiolate moiety, the Cu^{2+} ions from BSA@AuAg-Cu^{2+} system was unable to interact with TCh thus leading to quenching of BSA@AuAg NC (Path II) [Figure 3B, 4A(iv)].

3.3. Optimization of reaction parameters for ethyl parathion biosensor development

From the perspective of understanding proposed detection assay from change in fluorescence intensities, it was observed that the initial fluorescence at 650 nm as exhibited by synthesized BSA@AuAg NC was “switched off” with the addition of Cu^{2+} ions. This effect is mainly due to photoinduced quenching mechanism as the excited electrons of the BSA@AuAg NC follow intersystem crossing (ISC) pathway owing to the paramagnetic behavior of Cu^{2+} thereby resulting in the quenching of the fluorescence [44]. The BSA@AuAg NC showed a linear trend in the decrease of fluorescence intensity and red shift with increase in concentration of Cu^{2+} from 9.76 µM to 10 mM with lowest LOD for Cu^{2+}

calculated out to be 184 nM (Figure 4B, ESI). The shift in wavelength towards red region was observed mainly due to aggregation of BSA@AuAg NC at higher concentration of Cu^{2+} ion. Further, the fluorescence quenching efficiency was observed to be in good agreement with consistent Cu^{2+} concentration change having correlation coefficient, $R^2 = 0.9968$ (Figure 4C). Interestingly, conspicuous decrease in fluorescence intensity of BSA@AuAg NC was observed under UV light with the addition of Cu^{2+} ions (Figure 4C inset). Thus, for the further assay development, 5mM concentration of the Cu^{2+} was used as the optimized concentration.

AChE is polymeric glygoprotein having quaternary structure and is highly vulnerable for its denaturation in extreme pH conditions. Therefore, pH plays a crucial role for the detection of ethyl parathion using proposed assay. It was observed that in acidic conditions (between pH 4-6), the nanoprobe showed the aggregation behaviour (Figure. S3). This is mainly due to the change in the conformation of proteins at pH near to their isoelectric point (pI) as the pI of both BSA protein and AChE enzyme is in acidic range i.e. at 4.8 and 5.6, respectively [45, 46]. It is clearly visible from the graph [Fig. S4 (B)] that the fluorescence intensity of the BSA@AuAg NC attains stability between pH 7-8. Therefore, the catalytic activity of AChE enzyme has been studied at physiological pH (7.4).

The thiocholine (TCh) generation due to hydrolysis of ATCh using AChE enzyme is a crucial step for the proposed detection assay of ethyl parathion. In this context, controlled studies are required to determine the minimum concentration of both ATCh and AChE that has negligible effect on the fluorescence intensity of BSA@AuAg NC. The effect of increasing concentration of ATCh (from 10 to 500 µM) was thoroughly investigated on the fluorescence intensity of BSA@AuAg NC for every 10 min for 1 h. Specifically, as the concentration of ATCh exceeded 20 µM, the BSA@AuAg NC showed aggregation induce emission behaviour leading to persistent increase in the intensity of the BSA@AuAg NC (Figure 4D).

Correspondingly, 15 µM of ATCh was taken as optimal concentration for further studies. In a similar manner, the effect of AChE concentration on fluorescence intensity of BSA@AuAg NC was carried out at different time interval to determine the optimal time of hydrolysis reaction. It was observed that the hydrolysis rate become constant after 30 min of incubation (Figure S4). It was observed that at 300 mU/mL concentration of AChE, the fluorescence intensity of BSA@AuAg NC was not much altered and was chosen as controlled condition for further assay.

3.4. Investigation into sensitivity profile of the developed assay

One of the important aspects for qualitatively understanding the performance of developed sensing assay is by analysing the sensitivity of the developed nanoprobe for the determination of low-level concentration of ethyl parathion. In this regard, the sensitivity of the developed sensor was measured through variation in fluorescence signal of BSA@AuAg NC obtained as the concentration of ethyl parathion was varied from 5 to 10^6 pM. As expected, the fluorescence signal of NC gradually diminished with the increase in concentration of ethyl parathion owing to significant inhibition of enzymatic activity of AChE (Path II) (Figure 4E). To further check the robustness of the developed nanoprobe, the quenching efficiency (F_0/F-1) was plotted against the logarithm of each ethyl parathion concentration. A good correlation with respect to ethyl parathion concentration on fluorescence intensity of BSA@AuAg NC was obtained with correlation coefficient of R^2=0.99 (Figure 4F). Further, the LOD of ethyl parathion was calculated to be 2.40 pM (Table 1) using the formula LOD = 3α/m, where m is the slope of the calibration curve and α is the standard deviation from the blank sample (ESI). The calculated LOD obtained from the developed assay was one of the least as compared to previously reported methods based on traditional techniques such as GC-MS, LC-MS and to

more recent ones based electrochemical, colorimetric, SERS and immunoassay approaches along with other fluorometric based methods employing distinct fluorophores (Table 1).

Recently, quantification of mixed pesticides has been reported to be carried out using QD-AChE aerogel with LOD of 0.97 pM for ethyl parathion, however, its fabrication, maintenance and calibration of microfluidic chip along with complex synthetic protocol for aerogel limit the applicability of this sensor [45]. Thus, the developed enzyme based assay utilizing bimetallic NC emerged as a promising sensing nanoprobe for the pico-molar level detection of ethyl parathion in a simple, rapid and cost effective manner.

3.5. Applicability of developed bio-sensor in water and food samples

To investigate the relevance and applicability of designed NC based ethyl parathion detection assay, the developed method was further analysed in both water and food based real samples. For this purpose, soil water was taken and subjected to filtration for removal of suspended impurities whereas tap water was considered as such for analysis of the detection assay. Similarly, the orange and apple juice were taken and filtrated as food matrix samples. All these water and food samples were spiked with varied concentration of ethyl parathion at optimized parameters (Figure S5). As mentioned in Table 2, the clear observation was that the proposed nanoprobe, even in the presence of interfering ions, minerals, preservative and other components present in spiked water and food samples showed excellent comparable applicability. The percentage recovery varied in the range of 92 to 105 with more than acceptable R^2 value (0.95) in all tested real samples proving the appropriateness and accuracy of the developed assay.

3.6. Specificity analysis of developed bio-sensor

As mentioned earlier, the catalytic activity of the AChE enzyme is known to be blocked in the presence of OPs, therefore, it is significant to carry out specificity study of the developed nanoprobe in the presence of other pesticides (Figure S6). In this context, the developed assay was tested in presence of other commonly used OPs as well as non-organophosphorus pesticides including 2,4-D, atrazine, chlorosulfuron, and chloropyrifos along with ethyl parathion. It was observed that at a concentration of 1 nM, ethyl parathion showed the maximum inhibition for the AChE enzyme, while other tested pesticides (including chloropyrifos) were exhibiting comparably much lesser fluorescence quenching (Figure 5). The above results clearly demonstrated the specificity of the developed assay towards ethyl parathion.

4. CONCLUSION

In summary, a rapid and highly sensitive fluorometric biosensor for detection of ethyl parathion has been reported. The sensing strategy utilized the fluorometric responses of ultrasmall bimetallic AuAg NC to the modulation of ATCh-AChE concentration. Specifically, the proposed assay employed luminescent BSA@AuAg NC, synthesized using one pot green chemistry based biomineralization, which were made to interact with Cu^{2+} ions. This led to formation of BSA@AuAg NC-Cu^{2+} ensemble; resulting in quenching of NC's fluorescence. The addition of AChE along with ATCh resulted in generation of thiocholine (TCh) which is known to have preferable affinity with Cu^{2+} ions. As a consequence, fluorescence intensity of bimetallic NC was regained in the presence to *in situ* generated TCh. Upon further addition of ethyl parathion, a potential inhibitor to AChE enzyme, the fluorescence intensity of the solution was again 'turned off' due to relative non-formation of TCh. The 'on-off' fluorescence signals were evidently quite clear and could be easily quantified in absence as well as presence of ethyl parathion with LOD up to pico-molar range (2.40 pM) as the developed assay was highly sensitive.

The remarkably low sensitivity level of the present sensing platform is mainly the result of the following considerations. First and foremost, the fluorometric technique on which the sensing platform is based has proven to be more sensitive keeping in view of measurement of emission signal above low-level background and its path independent nature as compared to bright reference beam in absorbance-based technique. In addition, most of the photomultiplier tubes used in fluorescence-based sensing can easily detect low level of light and electronic impulses due to single photon measurement [27]. Secondly, bimetallic NC (BSA@AuAg) acting as a nanoprobe in this fluorescence-based sensing scheme, play a crucial role as the synergic effect of both atoms exhibits better performance in terms of electronic, catalytic and optical properties [39, 40]. The equally sensitive detection of Cu^{2+} ions upto 184 nM is mainly attributed due to indirect low level detection of analyte. Notably, this limit is much lower than the maximum contamination level (MCL) of Cu^{2+} in drinking water i.e. 1.3 mg/L [50]. Finally, the developed sensing method is based upon enzymatic modulated nanoprobe which is well known for its high sensitivity. The proposed biosensor inhibits the catalytic activity of AChE enzyme even in the presence of trace concentrations of ethyl parathion which is directly linked to the decrease in formation of catalytic product thiocholine (TCh). The generated TCh renders the quenching of fluorescence intensity of BSA@AuAg NC due to its preferential binding with Cu2+ ion.

To validate the developed dual biosensor, it was examined using real samples which exhibited excellent reproducibility and robustness even in the presence of other interfering substances. The specificity of the developed probe was also found in well agreement with spiked ethyl parathion concentration, with no significant interference observed in presence of other pesticides. It is pertinent to note here that the presently demonstrated enzyme-based fluorometric assay for ethyl parathion detection offer a clear advantage over other antibody as well as aptamer-based sensors in terms of its simplicity, rapidness, inexpensive nature and

high sensitivity. Thus, the developed assay using AChE coupled with metal NC provide a mode for the preliminary detection of ethyl parathion at minimal concentration of pM level. In addition, proposed assay finds a wide applicability for monitoring of even trace level of ethyl parathion in a rapid and cost-effective manner and further can open gateway for the sensing of other hazardous environmental pollutants. Encouraged by these results, it is safe to interpret that luminescent bimetallic BSA@AuAg NC have emerge as newer class of fluorophores that can be effectively utilized for various sensing platforms for even trace level concentration of analytes. In general, the bimetallic system is known to deliver better physical and optoelectronics properties over monoatomic system and metal NC specifically provides a much-needed alternative over other conventionally used fluorophores owing to their simpler synthetic protocol along with good quantum yield.

ACKNOWLEDGMENT

This study was supported by Science Education & Research Board (SERB) of India (grant F. No. EMR/2016/007967) and DST-PURSE II grant of India.

References

1. J. Popp, K. Peto, J. Nagy, Pesticide productivity and food security. A review Agron. Sustain. Dev. 3 (2013) 243–255.
2. R. Mesnage, G. E. Seralin, Editorial: Toxicity of pesticide on health and environment, Frontier in public health 6 (2018) 268.
3. A. Karunarathne, D. Gunnell, F. Konradsen, M. Eddleston, How many premature deaths from pesticide suicide have occurred since the agricultural Green Revolution? Clinical Toxicology (2019). doi.org/10.1080/15563650.2019.1662433.

4. US-EPA Fact sheet for ethyl parathion, 2000.
5. M.B. Olovi, D. Z. Krsti, T.D. Lazarevi, A. M. Bondi, V.M. Vasi, Current Neuropharmacology 11 (2013) 315-335.
6. N.L. Swanson, A. Leu, J. Abrahamson, B. Wallet, Genetically engineered crops, glyphosate and the deterioration of health in the United States of America, J. Org Syst. 9 (2014) 6–37.
7. https://ec.europa.eu/food/plant/pesticides/max_residue_levels/eu_rules_en.
8. R. Bala, S. Dhingra, M. Kumar, K. Bansal, S. Mittal, R. K. Sharma, N. Wangoo, Detection of organophosphorus pesticide-Malathion in environmental samples using peptide and aptamer, Chemical Engineering Journal 311 (2017) 111-116.
9. S. Xiong, Y. Deng, Y. Zhou, D. Gong, Y. Xu, L. Yang, H. Chen, L. Chen, T. Song, Current progress in biosensors for organophosphorus pesticides based on enzyme functionalized nanostructures: a review, Anal. Methods 10 (2018) 5468-5479.
10. R. Ramachandran, T.S. Chen, S.M. Chen, T. Baskar, R. Kannan, P. Elumalai, P. Raja, T. Jeyapragasam, K. Dinakaranh, G. Peter, G. Kumar, A review of the advanced developments of electrochemical sensors for the detection of toxic and bioactive molecules, Inorg. Chem. Front. 6 (2019) 3418-3439.
11. A. Sassolas, B. P. Simón, J. L. Marty, Biosensors for Pesticide Detection: New Trends, American Journal of Analytical Chemistry 3 (2012) 210-232.
12. D. Harshit, K. Charmy, P. Nrupesh, Organophosphorus pesticides determination by novel HPLC and spectrophotometric method, Food Chemistry 230 (2017) 448-453.
13. R, P. Lopes, F. A. S. Oliveira, F. D. Madureira, M. L. G. Oliveira, G. Silva, Multiresidue analysis of pesticide in peanuts using modified QuCHERS sample preparation and liquid chromatography-mass spectrometry detection, Anal. Methods 7 (2015) 4734-4739.

14. S. Soares, T. Castro, T. Rosado, N. Fernández, M. Barroso, E. Gallardo, New analytical approach to determine organophosphorus insecticides in blood by dried matrix spots sampling and GC-MS/MS, Anal. Bioanal. Chem. 410 (2018) 7955–7964.
15. C. A. D. Lima, R. Santana, J. V. Piovesan, A. Spinelli, Silver nanoparticle-modified electrode for the determination of nitro compound-containing pesticides, Anal. Bioanal. Chem. 408 (2016) 2595–2606.
16. A. Bu□a, D. Mandler, Adsorption and detection of organic pollutants by fixed bed carbon nanotube electrochemical membrane, Chemical Engineering Journal 359 (2019) 130–137.
17. B. J. Sanghavi, G. Hirch, S. P. Karna, A. K. Srivastava, Potentiometric stripping analysis of methyl and ethyl parathion employing carbon nanoparticles and halloysite nanoclay modified carbon paste electrode, Analytica Chimica Acta 735 (2012), 37-45.
18. Y. Bakytkarim, S. Tursynbolat, Q. Zeng, J. Huang, L. Wan, Nanomaterial ink for on-site painted sensors on studies of the electrochemical detection of organophosphorus pesticides residual of supermarket vegetable, Journal of Electroanalytical Chemistry 841 (2019) 45–50.
19. Y. Han, S. Liu, B. Liu, C. Jiang, Z. Zhang, In situ loading of Ag nanocontacts: A SERS platforms for ultrasensitive detection, RSC Adv. 4 (2014) 2776.
20. N. M. Dissanayakea, J. S. Arachchilagea, T. A. Samuelsa, S. O. Obarea, Highly sensitive plasmonic metal nanoparticle-based sensors for the detection of organophosphorus pesticides, Talanta, 200 (2019**)** 218–227.
21. R. Bala, S. Mittal, R. K. Sharma, N. Wangoo, A supersentive silver nanoprobe based aptasensor for low cost detection of malathion residue in water and food samples, Spectrochimica Acta Part A: Molecular and Biomolecular 196 (2018) 268–273.

22. R. Bala, M. Kumar, K. Bansal, R. K. Sharma, N. Wangoo, Ultrasensitive aptamer biosensor for malathion detection based on cationic polymer and gold nanoparticles, Biosensors and Bioelectronics 85 (2016) 445-449.

23. R. Bala, R.K. Sharma, N. Wangoo, Development of gold nanoparticles-based aptasensor for the colorimetric detection of organophosphorus pesticide phorate, Anal. Bioanal. Chem. 408 (2016) 333-338.

24. R. Bala, R. K. Sharma, N. Wangoo, Highly sensitive colorimetric detection of ethyl parathion using gold nanoprobes, Sensors and Acutaors B: Chemical 210 (2015) 425-430.

25. Y. Q. Zhang, Z. L. Xu, F. Wang, J. Cai, J. X. Dong, J. R. Zhang, R. Si, C. L. Wang, Y. Wang, Y. D. Shen, Y. Sun, H. Wang, Isolation of Bactrian Camel Single Domain Antibody for Parathion and Development of One-Step dc-FEIA Method Using VHH-Alkaline Phosphatase Fusion Protein, Anal. Chem. 90 (2018) 12886−12892.

26. L. Viveros, S. Paliwal, D. McCrae, J. Wild, A. Simonian, A fluorescence-based biosensors for the detection of organophosphorus pesticide and chemical warfare agent, Sensors and Acutators B: Chemical 115 (2006) 150-157.

27. J. R. Lakowicz (eds) Fluorescence Sensing. Principles of Fluorescence Spectroscopy, Springer, Boston, MA, 2006.

28. W. Deng, P. Chen, P. Hua, Z. Hea, M. Zhang, X. Yuan, K. Huan, Enzymatic reaction modulated synthesis of quantum dots for visual detection of cholinesterase activity and inhibiton, Sensors & Actuators: B. Chemical 292 (2019) 180–186.

29. R. Bala, A. Swami, I. Tabujew, K. Peneva, N. Wangoo, R. K. Sharma, Ultra-sensitive detection of malathion using quantum dots-polymer based fluorescence aptasensors, Biosensors and Bioelectronics 104 (2018) 45-49.

30. S.V. Carneiroa, V.H.R. De, A.A.C. Queiroza, L.M.U.D. Cruza, J.C. Fechinea, R.M. Denardin, R.F. Freireb, Sensing strategy based on Carbon Quantum Dots obtained from riboflavin for the identification of pesticides, Sensors & Actuators: B. Chemical 301 (2019) 127149.
31. Y. Zheng, L. Lai, W. Liu, H. Jiang, X. Wang, Recent advances in biomedical applications of fluorescent gold nanoclusters, Advances in colloidal and Interfaces Science 242 (2017) 1-16.
32. I. Chakraborty, T. Pradeep, Atomically Precise Clusters of Noble Metals: Emerging Link between Atoms and Nanoparticles, Chem. Rev. 117 (2017) 8208−8271.
33. J. Xie, Y. Zheng, J. Y. Ying, Protein-Directed Synthesis of Highly Fluorescent Gold Nanoclusters J. Am. Chem. Soc. 131 (2009) 888-889.
34. Y. B. Yin, C.L. Coonrod, K. N. Heck, F. Lejarza, M. S. Won, Microencapsulated Photoluminescent Gold for ppb-Level Chromium (VI) Sensing, ACS Appl. Mater. Interfaces 11 (2019) 17491−17500.
35. J. Meng, S. E, X. Wei, X. Chen, J. Wan, Confinement of AuAg NCs in a Pomegranate-Type Silica Architecture for Improved Copper Ion Sensing and Imaging, ACS Appl. Mater. Interfaces 11 (2019) 21150−21158.
36. Y. Tao, M. Li, J. Rena, X. Qu, Metal nanoclusters: novel probes for diagnostic and therapeutic application, Chem. Soc. Rev. 44 (2015) 8636.
37. N. Zhang, Y. Si, Z. Sun, L. Chen, R. Li, Y. Qiao, H. Wang, Rapid, Selective, and Ultrasensitive Fluorimetric Analysis of Mercury and Copper Levels in Blood Using Bimetallic Gold−Silver Nanoclusters with “Silver Effect”-Enhanced Red Fluorescence, Anal. Chem. 86 (2014) 11714−11721.

38. R. Jin, C. Zeng, M. Zhou, Y. Chen, Atomically Precise Colloidal Metal Nanoclusters and Nanoparticles: Fundamentals and Opportunities Chem. Rev. 116 (2016) 10346−10413.

39. Q. Zhai, H. Xing, X. Zhang J. Li, E. Wang, Enhanced Electrochemiluminescence Behavior of Gold–Silver Bimetallic Nanoclusters and Its Sensing Application for Mercury (II), Anal. Chem. 89 (2017) 7788-7794.

40. Q. Zhou, Y. Lin, M. Xu, Z. Gao, H. Yang, D. Tang, Facile Synthesis of Enhanced Fluorescent Gold–Silver Bimetallic Nanocluster and Its Application for Highly Sensitive Detection of Inorganic Pyrophosphatase Activity, Anal. Chem. 17 (2016) 8886-8892.

41. P. L. Xavier, K. Chaudhari, A. Baksi, T. Pradeep, Protein-protected luminescent noble metal quantum clusters: an emerging trend in atomic cluster nanoscience, Nano Reviews 3 (2012) 14767.

42. R. Gui, H. Jin, Aqueous synthesis of human serum albumin-stabilized fluorescent Au/Ag core/shell nanocrystals for highly sensitive and selective sensing of copper(ii), Analyst, 138 (2013) 7197−7205.

43. R.G. Pearson Absolute electronegativity and hardness: application to inorganic chemistry, Inorganic chemistry 31 (1988) 2797-2799.

44. V. Volchkov, V. L. Ivanov, B. M. Uzhinov, Induced Intersystem Crossing at the Fluorescence Quenching of Laser Dye 7-Amino-1,3-Naphthalenedisulfonic Acid by Paramagnetic Metal Ions, *J.* Fluoresc. 20 (2010) 299–303.

45. 43. H. Xiong, W. Wang, J. Liang, W. Wen, X. Zhang, S. Wang, A convenient purification method for metal nanoclusters based on pH-induced aggregation and cyclic regeneration and its applications in fluorescent pH sensors, Sensors and Actuators B 239 (2017) 988–992.

46. 44. M.C Jhu, Y.B. Xin, M.J Sun, Y.Z. Fang, Purification and properties of acetylcholinesterase from human brain, Sci China B. 1993 36(1993) 1207-1215.

47. L. Wei, X. Huang, F. Yan, L. Zheng, J. Wang, L. Xie, Y. Ya, Al-Doped Mesoporous Cellular Foam Modified Electrode as Sensor for the Detection of Parathion Pesticide, Int. J. Electrochem. Sci. 14 (2019) 1986 – 1996.

48. G. Hen, M. Jin, M. Yan, X. Cui. Y. Wang, W. Zheng, G. Qin, Y. Zhang, M. Li, Y. Liao, X. Zhang, F. Yan, J. Wang, Colorimetric bio-barcode immunoassay for parathion based on amplification by using platinum nanoparticles acting as a nanozyme, Microchim Acta 186 (2019) 339–348.

49. T. Hu, J. Xu, Y. Ye, Y. Han, X. Lia, Z. Wang, D. Sun, Y. Zhou, Z. Ni, Visual detection of mixed organophosphorous pesticide using QD-AChE aerogel based microfluidic arrays sensor, Biosensors and Bioelectronics 136 (2019) 112–117.

50. www.epa.gov/ground-water-and-drinking-water/national-primary-drinking-water-regulations

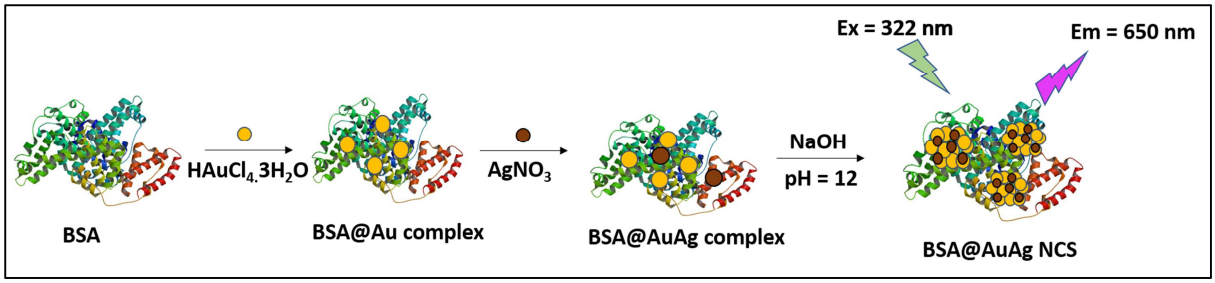

Figure 1. Schematic illustration for the synthesis of BSA@AuAg NC

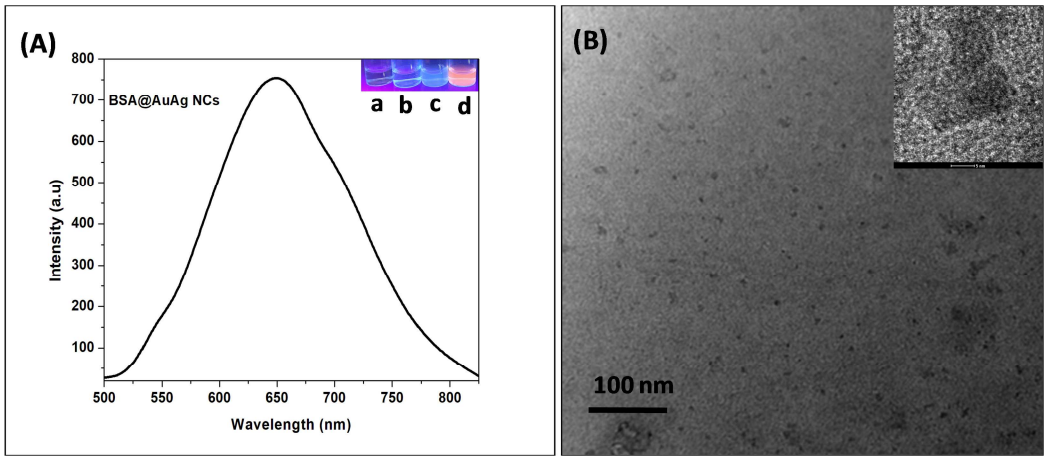

Figure 2. (A) Emission spectrum of BSA@AuAg NC upon excitation of 322 nm [inset: (a) $HClO_4$, (b) $AgNO_3$, (c) BSA and (d) BSA@AuAg NC image; under UV light] (B) TEM image of BSA@AuAg NC at scale bar of 100 nm (inset HR-TEM image at scale bar of 5 nm).

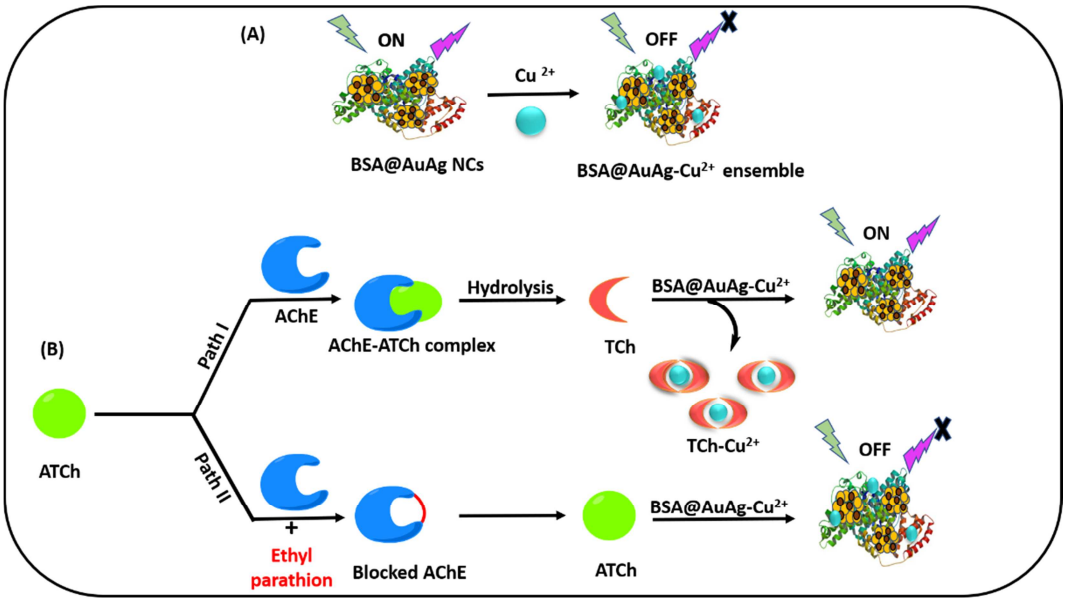

Figure 3. Schematic representation for the detection of ethyl parathion BSA@AuAg NC: (A) quenching of fluorescence intensity of BSA@AuAg NC in the presence of Cu^{2+} ions; (B) re-emergence of fluorescence intensity of BSA@AuAg NC in the presence of TCh or absence of ethyl parathion (path I) and quenching of fluorescence intensity of BSA@AuAg NC in the presence of ethyl parathion (path II).

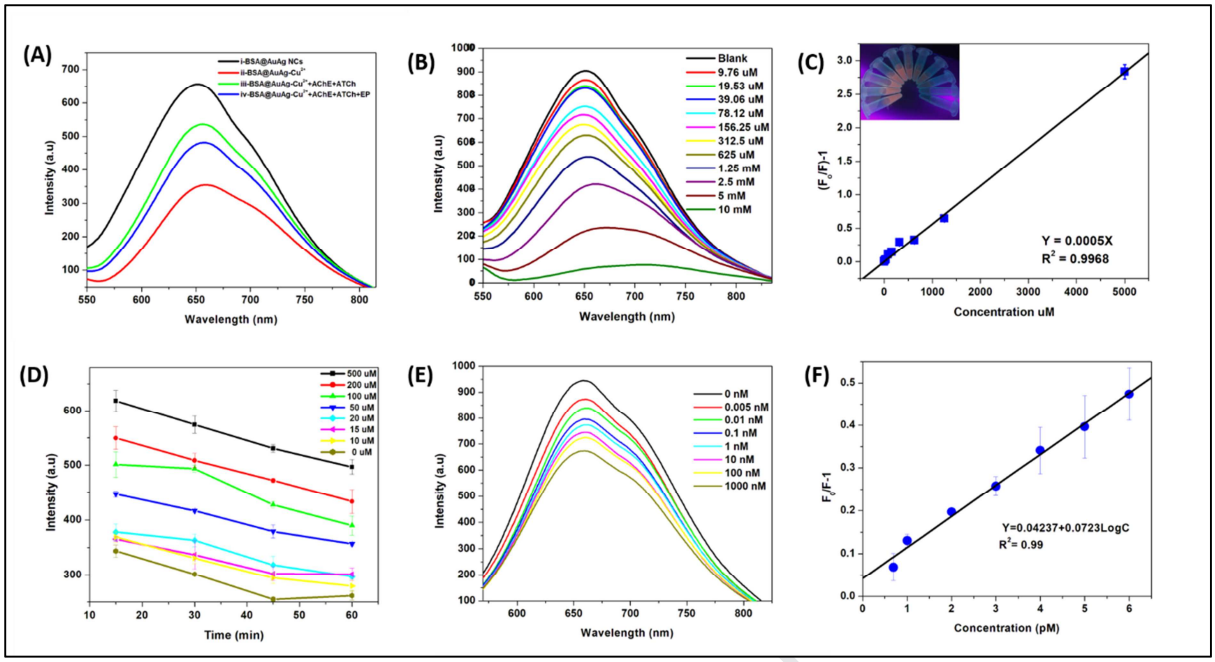

Figure 4. (A) Fluorescence spectra of (i) BSA@AuAg NC; (ii) BSA@AuAg NC after addition of Cu^{2};(iii) BSA@AuAg NC after addition of Cu^{2}, AChE and ATCh; (iv) BSA@AuAg NC after addition of Cu^{2+} AChE, ATCh and ethyl parathion (10 pM, 100 µL); **(B)** Fluorescence spectra of BSA@AuAg NC in the presence of Cu^{2+} ions (9.76-10000 µM); **(C)** Fluorescence quenching curve versus concentration of Cu^{2+} ion (inset image: BSA@AuAg NC in presence of Cu^{2+} ions under UV illuminator); **(D)** Variation of I_{650} of BSA@AuAg NC with time in the presence of ATCh (10-500 µM); **(E))** Fluorescence spectra of BSA@AuAg NC in the presence of ethyl parathion (0.005-1000 nM); **(F)** Fluorescence quenching efficiency curve versus concentration of ethyl parathion.

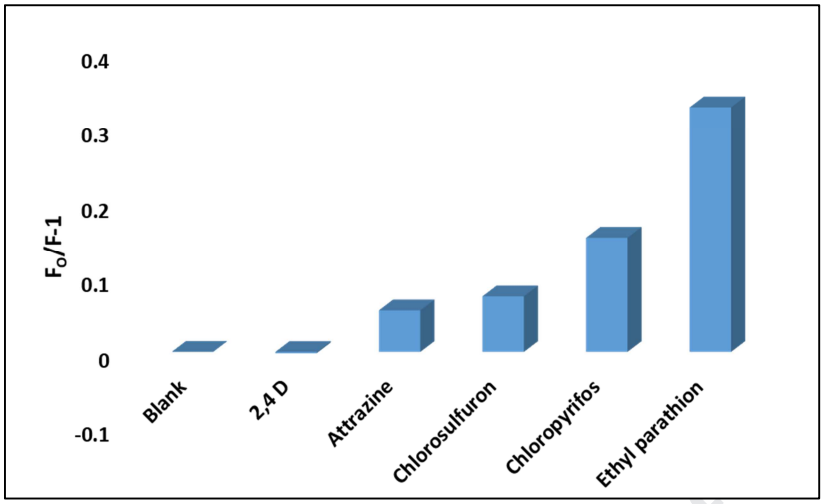

Figure 5. Fluorescence response of BSA@AuAg NC towards different OPs and other pesticides (concentration of all pesticides was taken as 1 nM whereas concentration of Cu^{2+}, AChE and ATCh were taken as 5 mM, 300 mU/mL and 15 µM respectively; F_o and F represent the fluorescence intensities in the absence and presence of pesticide, respectively)

Table 1. LOD values for ethyl parathion detection based on already reported methods/techniques as compared to the present method

Technique Used/substrate	LOD (concentration)	Reference
GC-MS/MS	3.44 µM	14
Surface enhanced Raman Scattering (SERS)	10 µM	19
Electrochemical	0.54 nM	47
Colorimetric assay	0.27 nM	24
Colorimetric immunoassay	2.8 pM	48
Direct-Fluorescence ELISA immunoassay	0.68 nM	25
Fluorometric based Quantum dots	0.325 nM	27
Fluorometric based Carbon dots	858.2 nM	29
QD-AChE aerogel microfluidic chip	0.97 pM	49
Fluorometric based bimetallic NC	*2.40 pM*	*Present work*

Table 2. Percentage recovery obtained for detection of the ethyl parathion in spiked water and food samples using the designed assay

Sample type	Regression Coefficient (R^2)	Spiked Amount (nM)	Amount found (nM)	Recovery %
Tap water	0.97	1	1.03	103
		100	93	93
Soil water	0.97	1	1.02	102
		100	96	96
Orange juice	0.98	1	1.03	103
		100	99	99
Apple juice	0.95	1	1.05	105
		100	92	92

Highlights

- One pot rapid green synthesis of bimetallic nanoclusters using BSA as a scaffold (BSA@AuAg NC).
- Development of dual biosensor by utilizing enzymatic reaction of acetylthiocholine for the detection of ethyl parathion and Cu^{2+} ions.
- BSA@AuAg NC showed fluorescence quenching in the presence of Cu^{2+} ions, exhibiting LOD of 184 nM.
- Ultrasensitive detection of ethyl parathion using NC-enzyme probe with LOD value up to 2.40 pM was calculated.
- The LOD noted for bio-sensing of ethyl parathion is one of lowest reported in the literature so far across different techniques.
- The proposed assay depicted good relevancy and robustness in real samples along with tested non-interference analysis with other pesticides.

Highlights

- One pot rapid green synthesis of bimetallic nanoclusters using BSA as a scaffold (BSA@AuAg NC).
- Development of dual biosensor by utilizing enzymatic reaction of acetylthiocholine for the detection of ethyl parathion and Cu^{2+} ions.
- BSA@AuAg NC showed fluorescence quenching in the presence of Cu^{2+} ions, exhibiting LOD of 184 nM.
- Ultrasensitive detection of ethyl parathion using NC-enzyme probe with LOD value up to 2.40 pM was calculated.
- The LOD noted for bio-sensing of ethyl parathion is one of lowest reported in the literature so far across different techniques.
- The proposed assay depicted good relevancy and robustness in real samples along with tested non-interference analysis with other pesticides.